

Electronic Supplementary Information

Soft nanocomposites of lead bromide perovskite and polyurethane prepared via coordination chemistry for highly flexible, stable, and quaternary metal alloy-printed light emitting diodes

Ga Eun Kim, Hae-Jin Kim, Heesuk Jung, and Minwoo Park*

G. E. Kim and Prof. M. Park

Department of Chemical and Biological Engineering
Sookmyung Women's University, Seoul, 04310, Korea

Prof. H.-J. Kim

School of Mechanical Engineering,
Yonsei University, Seoul, 03722, Korea

Dr. H. Jung

Advanced Photovoltaics Research Center,
Korea Institute of Science and Technology (KIST), Seoul, 02792, Korea

*Corresponding author: M. Park (mwpark@sm.ac.kr)

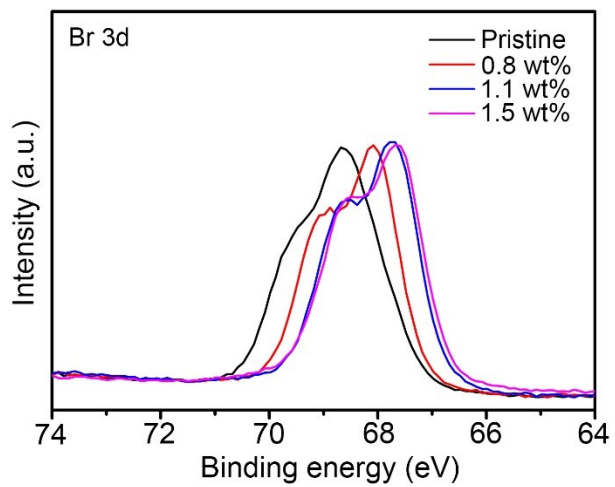


Figure S1. Br 3d X-ray photoelectron spectra of MAPbBr₃-DMSO and MAPbBr₃-PU-DMSO complex films.

Table S1. Time-resolved photoluminescence parameters of perovskite deposited onto glass/ITO/PEDOT:PSS substrates fitted using biexponential decay function.^{a)}

PU concentration [wt%]	a ₁	τ ₁ [ns]	a ₂	τ ₂ [ns]	τ _{avg} [ns] ^{b)}
0	0.734	14.03	0.266	64.23	27.38
0.8	0.749	15.94	0.251	114.1	40.58
1.1	0.716	14.98	0.284	135.6	49.24
1.5	0.705	16.67	0.295	177.4	64.09

^{a)}Fit function = $a_1 e^{-t/\tau_1} + a_2 e^{-t/\tau_2}$

^{b)} $\tau_{avg} = (\sum_i a_i \tau_i) / (\sum_i a_i)$, where $\sum_i a_i = 1$

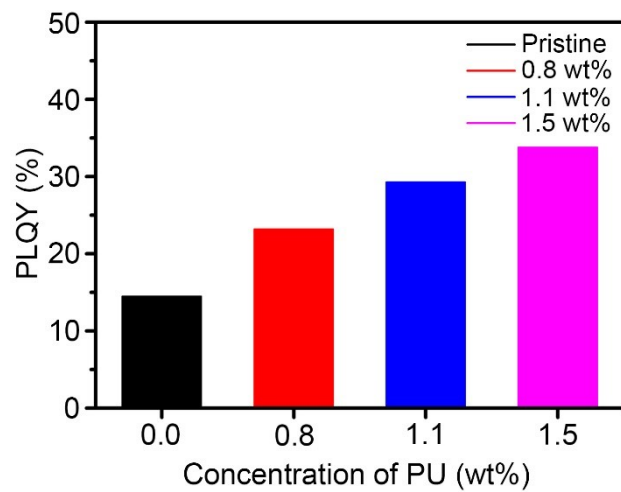


Figure S2. PLQYs of MAPbBr₃ and MAPbBr₃-PU films.

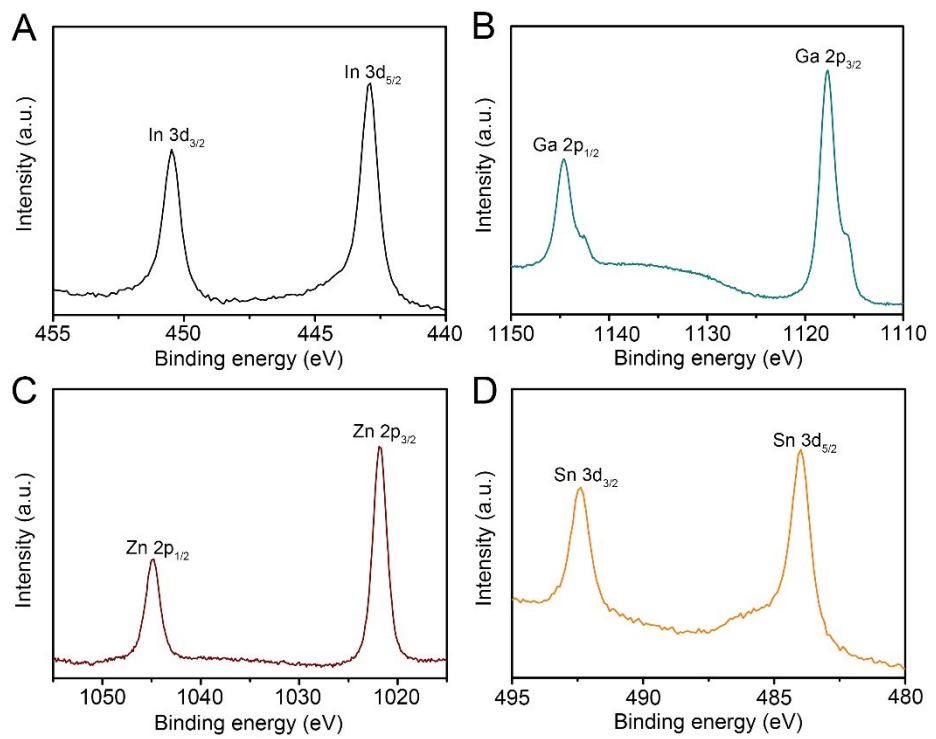


Figure S3. X-ray photoelectron spectra of IGZS displaying (A) In 3d, (B) Ga 2p, (C) Zn 2p, and (D) Sn 3d.

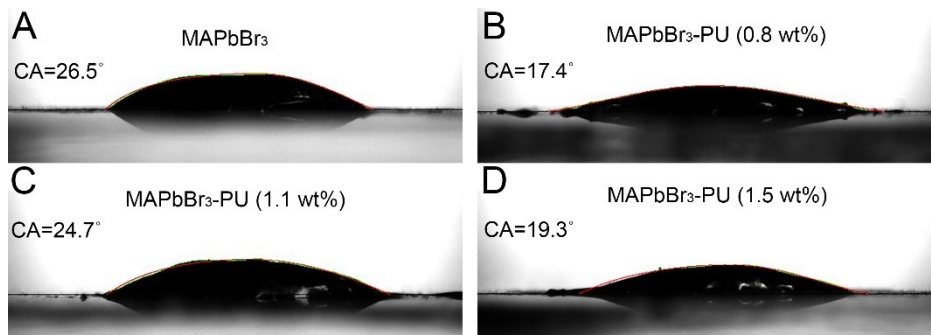


Figure S4. Optical microscopy images of IGZS droplets on (A) glass/ITO/PEDOT:PSS/MAPbBr₃/PCBM, (B) glass/ITO/PEDOT:PSS/MAPbBr₃-PU0.8/PCBM, (C) glass/ITO/PEDOT:PSS/MAPbBr₃-PU1.1/PCBM, and (D) glass/ITO/PEDOT:PSS/MAPbBr₃-PU1.5/PCBM.

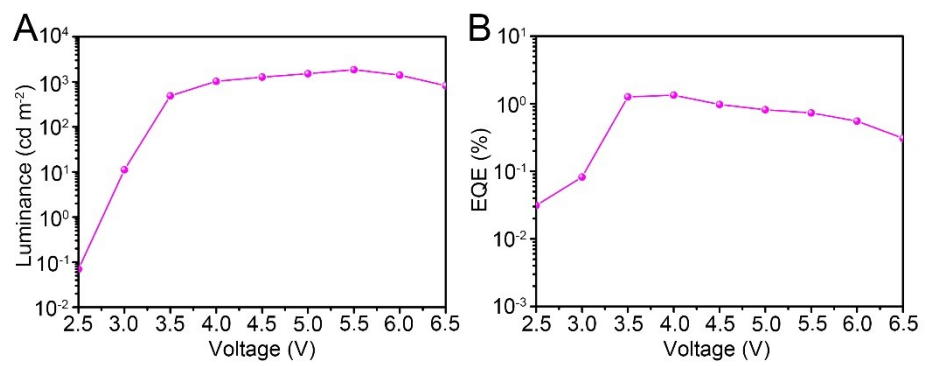


Figure S5. (A) Luminance–voltage and (B) EQE–voltage curves of MAPbBr₃-PU1.5 device with Ag NW cathode.

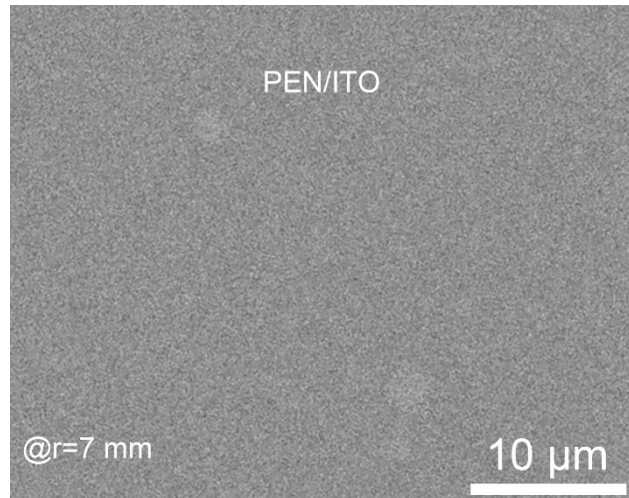


Figure S6. SEM image of PEN/ITO substrate at $r = 7$ mm.

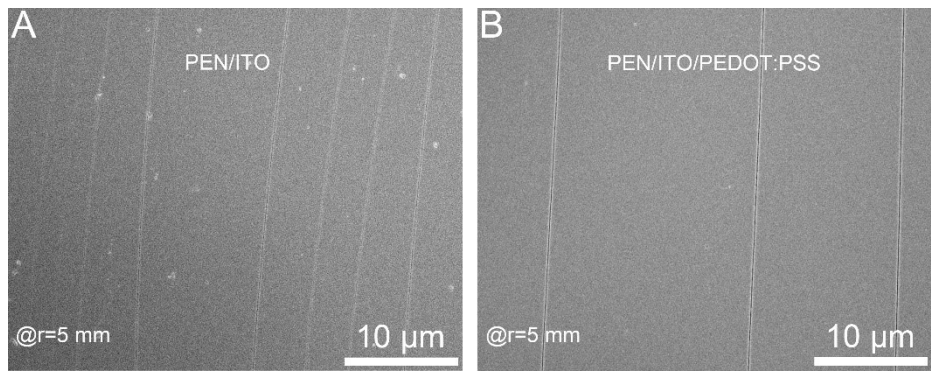


Figure S7. SEM images of (a) PEN/ITO and (b) PEN/ITO/PEDOT:PSS substrates at $r = 5$ mm.

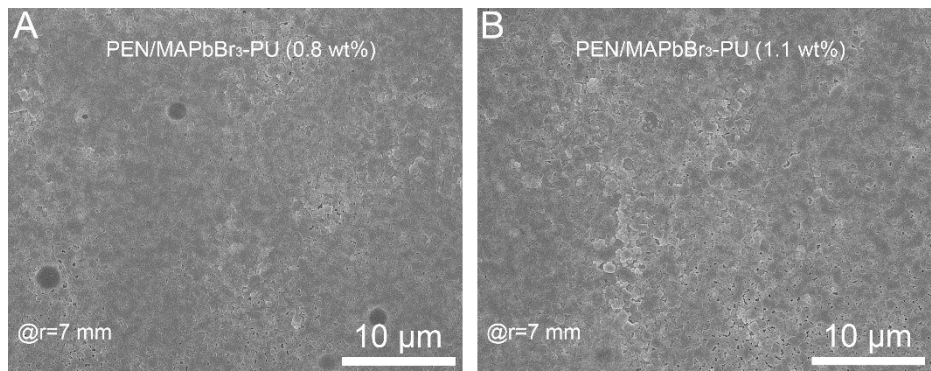


Figure S8. SEM images of (a) PEN/MAPbBr₃-PU0.8 and (b) PEN/MAPbBr₃-PU1.1 substrates at $r = 7$ mm.

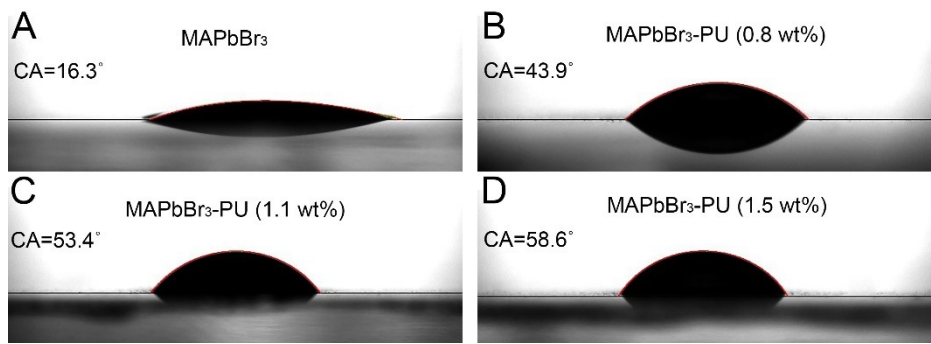


Figure S9. Optical microscopy images of water droplets on (A) glass/ITO/PEDOT:PSS/MAPbBr₃, (B) glass/ITO/PEDOT:PSS/MAPbBr₃-PU0.8, (C) glass/ITO/PEDOT:PSS/MAPbBr₃-PU1.1, and (D) glass/ITO/PEDOT:PSS/MAPbBr₃-PU1.5.

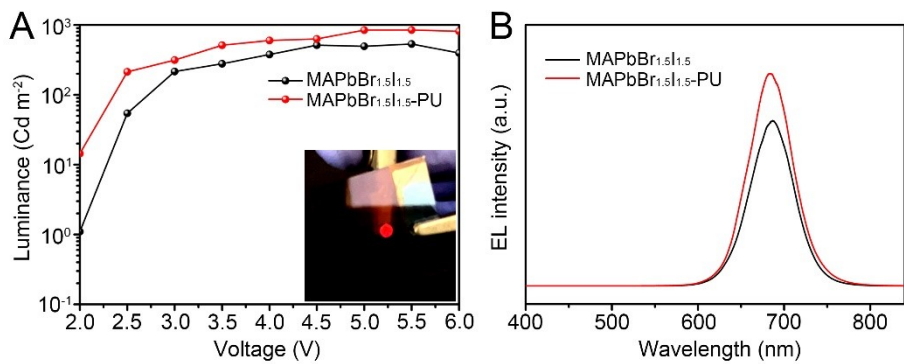


Figure S10. (A) Luminance-voltage and (B) EL spectra of MAPbBr_{1.5}I_{1.5} and MAPbBr_{1.5}I_{1.5}-PU devices. The inset photograph exhibits the working device at 2.5V. The EL peaks are observed at 689.4 nm.

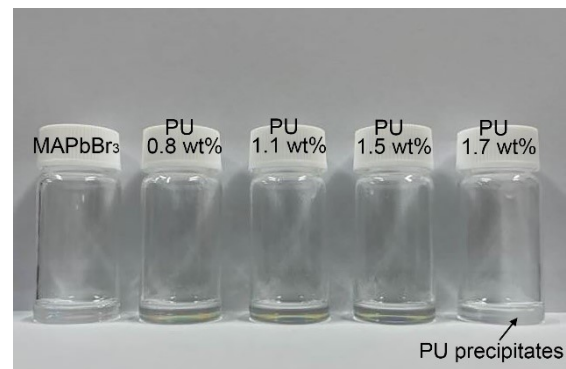


Figure S11. Photographs of MAPbBr₃ and MAPbBr₃-PU (0.8, 1.1, 1.5, and 1.7 wt%) solutions.

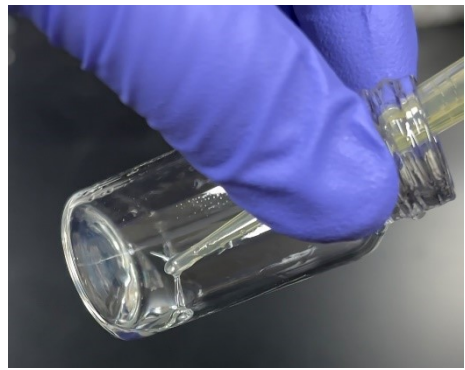


Figure S12. Magnified photograph of MAPbBr₃-PU (1.7 wt%) solution. The PU precipitates form a large lump, separated from the solution.